Transport properties of electron swarms in gaseous neon at low values of E/N

G. J. Boyle, M. J. E. Casey, and R. D. White
School of Engineering and Physical Sciences, James Cook University, Townsville Queensland 4810, Australia

Y. Cheng and J. Mitroy
School of Engineering, Charles Darwin University, Darwin Northern Territory 0909, Australia
(Dated: May 16, 2014)

A detailed analysis of electron swarm transport through neon gas at applied reduced electric fields of $E/N < 2$ Td is presented. The root mean square difference of transport parameters calculated from a recent all-order many-body perturbation theory treatment (Y. Cheng *et al.*, Phys. Rev. A **891**, 012701 (2014)) with drift velocity measurements by the Australian National University group (A. G. Robertson, J. Phys. B **5**, 648 (1972)) is less than 1%. Differences of about 3% exist with characteristic energies, D_T/μ, (T. Koizumi *et al.*, J. Phys. B 17, 4387 (1984)) indicating an incompatibility at the 3% level between drift velocity and transverse diffusion coefficient measurements. Multi-term solutions of the Boltzmann equation indicate that the two-term approximation gives transport parameters accurate to better than 0.01%. Attention was paid to the numerical representation of the cross section. A recommended elastic momentum transfer cross section has been constructed that has a maximum difference of 0.5% with all ANU drift velocity data for $E/N < 1.6$ Td and a root mean square difference that is about a factor of 2 smaller.

PACS numbers: 34.85.+x, 34.80.Bm, 31.25.Jf, 03.65.Nk,51.50.+v; 52.25.Fi;

I. INTRODUCTION

The electron-helium system is the most thoroughly investigated electron-atom collision system. There have been numerous experiments and calculations that have studied practically every important reaction channel for this system [1–4]. The quality of agreement between theory and experiment is now very good and for many practical applications the calculation of the electron-helium collision properties can be regarded as a solved problem. Indeed, electron-helium cross sections computed with the Kohn variational method at energies below the first excitation threshold are often adopted as a benchmark cross section [5, 6].

The present investigation is focussed on the electron-neon system. A recent study of electron-neon cross section sets concluded that they were adequate for the purposes of plasma modelling where an overall accuracy of 10% is needed [3]. Furthermore, it was noted that theoretical cross section sets from B-spline R-matrix calculations [3, 7, 8] could reproduce swarm parameters in good agreement with cross section over a range of E/N (where E is the applied electric field and N is the density of the neon gas) varying from 10^{-2} to 10^{3} Td [3]. Coincident with this work, a state of the art method for atomic structure, the relativistic all-order many body perturbation theory with single and double excitations (SDpT) [9, 10], was adapted to describe low energy electron neon scattering [11]. The derived cross sections were able to reproduce most existing elastic and momentum transfer cross section data to an accuracy of better than 5%.

Accordingly, it is now appropriate to perform a stringent analysis of the low energy cross section with particular emphasis on a detailed comparison with swarm experiments at low values of E/N. There have been measurements of the drift velocity, $v_{\rm dr}$, [12–16] and the characteristic energy (the ratio of the transverse diffusion coefficient D_T to the mobility $\mu = v_{\rm dr}/E$, D_T/μ) [17]. These measurements have been used to generate estimates of the momentum transfer cross section [15, 17–21]. Other transport parameters that have been measured include the diffusion coefficient at thermal energies [22–26] and the longitudinal diffusion coefficient [27].

In the present work, we initially introduce the cross section sets that are adopted and detail the procedure to compute the transport parameters. Attention is given to the fine details of the analysis such as the numerical representation of the cross section and the validity of the two-term solution to the Boltzmann equation [28, 29]. An assessment of a number of empirically derived momentum transfer cross sections is also made. Calculations provide evidence that the transverse diffusion coefficients measured by the Rikkyo group and the drift velocity measurements of the Australian National University (ANU) are incompatible at a level equivalent to 3% in the transport parameters.

II. CROSS SECTIONS

This work is reliant on three different types of low energy cross section. These are the elastic cross section, $\sigma_{\rm T}$, the momentum transfer cross section, $\sigma_{\rm MT}$, and the viscosity cross section, $\sigma_{\rm V}$. The viscosity cross section is needed for solutions of the Boltzmann equation that go beyond the two-term approximation (see Section III). All can be defined in terms of angular integrals of the differential cross section $\sigma(\theta)$ where θ is the scattering angle. Furthermore, expressions in terms of phase shifts

are also known. These cross sections are defined

$$\begin{aligned}\sigma_{\rm T} &= 2\pi\int\sigma(\theta)\ \sin(\theta)\ d\theta \\ &= \frac{4\pi}{k^2}\sum_{\ell=0}\left((\ell+1)\sin^2(\delta_\ell^+)+\ell\sin^2(\delta_\ell^-)\right), \quad (1)\end{aligned}$$

$$\begin{aligned}\sigma_{\rm MT} &= 2\pi\int(1-\cos\theta)\sigma(\theta)\ \sin(\theta)\ d\theta \\ &= \frac{4\pi}{k^2}\sum_{\ell=0}\Big(\frac{(\ell+1)(\ell+2)}{(2\ell+3)}\sin^2(\delta_\ell^+-\delta_{\ell+1}^+) \\ &+ \frac{\ell(\ell+1)}{(2\ell+1)}\sin^2(\delta_\ell^--\delta_{\ell+1}^-) \\ &+ \frac{(\ell+1)}{(2\ell+1)(2\ell+3)}\sin^2(\delta_\ell^+-\delta_{\ell+1}^-)\Big)\ . \quad (2)\end{aligned}$$

$$\begin{aligned}\sigma_V &= 2\pi\int(1-\cos^2\theta)\ \sigma(\theta)\ \sin(\theta)\ d\theta \\ &= \frac{4\pi}{k^2}\sum_{\ell=0}\Big(\frac{2\ell(\ell+1)}{(2\ell-1)(2\ell+1)(2\ell+3)}\sin^2(\delta_\ell^+-\delta_\ell^-) \\ &+ \frac{(\ell+1)(\ell+2)(\ell+3)}{(2\ell+3)(2\ell+5)}\sin^2(\delta_\ell^+-\delta_{\ell+2}^+) \\ &+ \frac{\ell(\ell+1)(\ell+2)}{(2\ell+1)(2\ell+3)}\sin^2(\delta_\ell^--\delta_{\ell+2}^-) \\ &+ \frac{2(\ell+1)(\ell+2)}{(2\ell+1)(2\ell+3)(2\ell+5)}\sin^2(\delta_\ell^+-\delta_{\ell+2}^-)\Big)\ . \quad (3)\end{aligned}$$

In these equations, δ_ℓ^+ refers to the phase shift with $j=\ell+\frac{1}{2}$ and δ_ℓ^- refers to the phase shift with $j=\ell-\frac{1}{2}$. The expression for the momentum transfer cross section is compatible with that previously given by McEachran [30].

The $\ell=0,1$ and 2 phase shifts were obtained from a recent calculation using relativistic many-body perturbation theory [11]. This SDpT calculation iterates many-body perturbation theory for an excitation space allowing for all possible single and double excitations until convergence is reached. The effects of triple excitations are included perturbatively [10].

The SDpT phase shifts cover an energy range from $k=0$ to $k=0.80\ a_0^{-1}$. These phase shifts are extended to higher energies using a central field model. The effective Hamiltonian (in atomic units) for the electron with coordinate $\mathbf{r}_0$ moving in the field of the atom is written

$$H=-\frac{1}{2}\nabla_0^2+V_{\rm dir}(\mathbf{r}_0)+V_{\rm exc}(\mathbf{r}_0)+V_{\rm pol}^{\ell,j}(\mathbf{r}_0)\ . \quad (4)$$

In Eq. (4), $V_{\rm dir}(\mathbf{r}_0)$ and $V_{\rm exc}(\mathbf{r}_0)$ are the direct and exchange interactions of the scattering electron with the neon target which is represented by a Hartree-Fock wavefunction. The angular momentum dependent polarization potential is given the form

$$V_{\rm pol}^{\ell,j}(\mathbf{r}_0)=-\frac{\alpha_d(1-\exp\left(-r_0^6/\rho_{\ell,j}^6\right))}{2r_0^4}, \quad (5)$$

where α_d is the static dipole polarizability which is set to 2.669 a_0^3 [11]. The adjustable parameters, $\rho_{\ell,j}$ are fixed by reference to the value of the phase shifts near $k\approx 0.80\ a_0^{-1}$.

Higher ℓ phase shifts are given by the modified effective range theory (MERT) formula [31–33],

$$\tan(\delta_\ell)=\frac{\pi\alpha_d k^2}{(2\ell-1)(2\ell+1)(2\ell+3)}\ . \quad (6)$$

The SDpT cross sections, with the model potential extension to higher energies are tabulated in the supplementary material [34]. The cross sections are tabulated on a dense momentum grid, with spacings of $\Delta k=0.001\ a_0^{-1}$ at the lowest momenta and a spacing of $\Delta k=0.01\ a_0^{-1}$ at the higher momenta. The net number of points in the tabulation is 139. A momentum grid provides a better representation of the variations in the cross section at low energies than a similarly sized energy grid.

One characteristic of the e^--neon $\sigma_{\rm MT}$ is its abnormally small size of $\approx 0.17\times10^{-20}$ m^2 at zero energy ($\epsilon=0$). The cross section increases rapidly as the energy increases and is about three times larger at thermal energies.

A. Cross section sets

Besides the present cross section set, there were two other theoretical cross section sets used to calculate the transport parameters. One set is the momentum transfer cross section from the *ab-initio* B-spline R-matrix (BSR) calculations [7, 8]. The basis used in this calculation was large. The BSR calculation does not report the viscosity cross section (or phase shifts) that would allow a solution of the Boltzmann equation to go beyond the two-term approximation. However, the BSR calculation gave elastic, excitation and ionization cross sections that extend to high energy and therefore can be used in simulations of electron transport at high E/N.

Another theoretical cross section is that from the multi-configuration Hartree-Fock (MCHF) calculations [35]. One limitation with the MCHF data is that the data is restricted to energies with $\epsilon\le 7$ eV and further only the elastic and momentum transfer cross sections are given. The MCHF $\sigma_{\rm MT}$ was set to its 7 eV value for all energies greater than 7 eV when solving the Boltzmann equation.

Other momentum transfer cross sections are essentially derived from experiment. The cross section of Robertson [15] was determined by solving the two-term Boltzmann equation and iteratively adjusting the momentum transfer cross section. The same approach was used by the Rikkyo group [17], except in this case the momentum transfer cross section was tuned by fitting to the characteristic energy D_T/μ. Another approach by O'Malley and Crompton used modified effective range theory (MERT) to help derive expressions of the scattering phase shifts at low energy [21] by fitting the ANU

drift velocity measurements. The scattering length derived from the O'Malley fit was $0.214 \pm 0.005\ a_0$. Most of the electron-Ne momentum transfer cross sections in the LXcat database [3, 36] incorporate elements of the Robertson [15] or O'Malley [21] $\sigma_{\rm MT}$.

The recommended cross section published by Buckman and Elford [37, 38] is an amalgam of the Robertson and O'Malley cross sections for $\epsilon < 4$ eV. The zero energy cross section of $0.163{\times}10^{-20}$ m^2 is slightly larger than that of O'Malley. At higher energies this cross section was derived from crossbeam measurements [39, 40] and the MCHF calculations [35, 41].

The cross section of Morgan [3, 42] is essentially the Buckman cross section up to 4 eV, but has omitted many energies from the Buckman tabulation below 0.03 eV. The Morgan cross section starts to deviate from the Buckman cross section for $\epsilon > 4$ eV.

The SIGLO database [3, 43, 44] uses the Robertson $\sigma_{\rm MT}$ [15] data from 0.03 to 6.0 eV. The zero energy cross section of 0.161×10^{-20} m^2 was computed using the O'Malley scattering length [21]. The cross section at energies greater than 6 eV is different from the Robertson cross section and is taken from Shimamura [45].

The Biagi $\sigma_{\rm MT}$ is stated to be taken from version 8.9 of the Magboltz Monte Carlo program [3, 46–48]. At low energies, the momentum transfer cross section is based on the MERT fitting formulae of O'Malley [21]. Examination of the source code of the Magboltz program indicates no values below 1 eV, but values below 1 eV are tabulated in the LXcat database. The $\epsilon = 0$ cross section was fixed to the value at 0.0001 eV, but this is about 8% larger than expected from the O'Malley scattering length.

The Puech data for neon was initially described in [49, 50]. It is stated that this cross section was taken from Robertson [15] for $\epsilon < 7$ eV while the cross section of Hayashi is used at higher energies. Examination of the tabulation reveals differences of a few percent with the Robertson $\sigma_{\rm MT}$ across the energy range for which Robertson tabulate the cross section.

A new empirical cross section was constructed from the SDpT by multiplying it by a simple energy dependent scaling factor of the form, $A = 1/(1+\alpha\exp(-\epsilon/\beta))$. The choice of $\alpha = 0.08$ and $\beta = 0.089$ eV gave a $\sigma_{\rm MT}$ that gave a superior fit to the ANU $v_{\rm dr}$ data for $E/N < 0.01$ Td. This cross section is identified in all subsequent text as the SDpTv2 cross section. The scattering length of the SDpTv2 cross section is $0.2158\ a_0$. The SDpTv2 cross sections are tabulated in the supplementary material [34].

All of the cross sections have been tested by computing drift velocities and transverse diffusion coefficients. Detailed comparisons of transport parameters computed with the SDpT, BSR, SDpTv2 and Buckman are given as a function of the applied reduced electric field, E/N. The Buckman cross section was chosen as a representative example of the empirically derived cross sections. Some summary assessments, e.g. the root mean square differences from experiment, where all cross sections are tested against available transport data are also made.

III. MULTI-TERM SOLUTION OF BOLTZMANN'S EQUATION

The transport of a swarm of electrons in neon driven out of thermal equilibrium by a low applied electric field can be described by the steady-state spatially homogeneous Boltzmann's equation for the velocity distribution function $f(\boldsymbol{v})$ [51]:

$$\frac{e\boldsymbol{E}}{m_e}\cdot\frac{\partial f}{\partial \boldsymbol{v}} = J(f,F)\ , \tag{7}$$

where $\boldsymbol{v}$ and e denote the velocity and charge of the electron respectively. The collision operator $J(f,F)$ takes into account binary interactions between the electrons of mass m_e and the neon atoms of mass M, where $F(\boldsymbol{V})$ denotes the background gas velocity ($\boldsymbol{V}$) distribution function, which is assumed to be Maxwellian at the gas temperature T. For the applied electric fields considered in this manuscript, the only scattering processes operative in neon are elastic in nature.

Solution of eq. (7) requires decomposition of $f(\boldsymbol{v})$ in velocity space through an expansion in Legendre polynomials:

$$f(\boldsymbol{v}) = \sum_{l=0}^{\infty} f^{(l)}(v) P_l(\cos\theta)\ , \tag{8}$$

where $P_l(\cos\theta)$ are Legendre polynomials and θ denotes the angle relative to the electric field direction (taken to be the z-axis). Setting the upper bound of the l-summation in eq. (8) to 1 leads to the well-known two-term approximation. This restriction assumes *a priori* that the velocity distribution is quasi-isotropic. In best practice, the integer $l_{\rm max}$ is successively incremented until a prescribed accuracy criterion is met and this is the avenue pursued in this study. This is a multi-term solution of Boltzmann's equation. Using the orthogonality of Legendre polynomials, combining eqs. (7) and (8) leads to the following system of coupled equations for $f^{(l)}$:

$$J^l f^{(l)} - \frac{eE}{m_e}\left\{\frac{l+1}{2l+3}\left[\frac{d}{dv}+\frac{l+2}{v}\right]f^{(l+1)} - \frac{l}{2l-1}\left[\frac{d}{dv}-\frac{l-1}{v}\right]f^{(l-1)}\right\} = 0. \tag{9}$$

For electrons in gaseous neon it is sufficient to exploit the small mass ratio and utilise the Davydov operator to describe elastic collisions:

$$J^0 f^{(0)} = \frac{m_e}{Mv^2}\frac{\partial}{\partial v}\left\{v\nu_m(v)\left[v f^{(0)} + \frac{k_B T}{m_e}\frac{\partial}{\partial v}f^{(0)}\right]\right\} \tag{10}$$

$$J^l f^{(l)} = \nu_l(v) f^{(l)} \qquad \text{for } l{\geq}1, \tag{11}$$

and

$$\nu_l(v) = N v 2\pi \int_0^{\pi} \sigma(v,\theta)\left[1 - P_l(\cos\theta)\right]\sin\theta d\theta. \tag{12}$$

We note for $l = 1$, $\nu_1 = \nu_m = Nv\sigma_{\rm MT}$ is the momentum transfer collision frequency for elastic collisions, while for $l = 2$, $\nu_2 = \nu_{\rm V} = \frac{3}{2}Nv\sigma_{\rm V}$ which samples the viscosity cross section. We enforce the normalisation condition:

$$4\pi \int_0^\infty f^{(0)}(v)v^2 dv = 1 \, . \tag{13}$$

Details of the numerical solution of the system of equations can be found in [52].

The measured drift velocity $v_{\rm dr}$ in this reduced field regime is related to the velocity distribution function via:

$$v_{\rm dr} = \frac{4\pi}{3} \int_0^\infty v f^{(1)}(v)v^2 dv, \tag{14}$$

while the mean energy of the electron swarm is given by:

$$\langle \epsilon \rangle = 4\pi \int_0^\infty \frac{1}{2} m_e v^2 f^{(0)}(v)v^2 dv. \tag{15}$$

Of note for this particular study, is the characteristic energy, defined as the ratio of the transverse diffusion coefficient D_T to the electron mobility $\mu (= v_{\rm dr}/E)$ [28]:

$$\frac{D_T}{\mu} = 0.1 \left(\frac{E}{N}\right)_{\rm Td} \frac{\int_0^\infty \frac{v}{\sigma_{\rm MT}} f^{(0)}(v)v^2 dv}{\int_0^\infty v f^{(1)}(v)v^2 dv}, \tag{16}$$

where the reduced electric field is in Townsend (Td) and $\sigma_{\rm MT}$ is in units of 10^{-20} m^2.

IV. COMPARISON WITH TRANSPORT DATA

Comparisons are made with four sets of experimental data. First there are the drift velocities of the ANU group [15]. Drift velocities at applied electric fields ranging from 0.001594 Td to 2.003 Td have been made at 77 K and 293 K. The stated uncertainty for this set of drift velocities is ±1%. In addition, there are the characteristic energies from the university of Rikkyo group [17]. They were obtained at 293 K using values of E/N ranging from 0.014 Td to 0.40 Td and are reported with a stated uncertainty of ±3%. Finally, the diffusion coefficient at thermal energies has been measured [23–26].

The mass of the neon atom in the solution of the Boltzmann equation was taken as 20.1797 amu [53].

A. Validity of the two-term approximation

Two different solutions of the Boltzmann equation were made using the SDpT cross section. One of the solutions was made using the two-term approximation. The other solution was a four-term solution which included the viscosity cross section, $\sigma_{\rm V}$. The differences in the drift velocity and diffusion coefficients due to the two-term and four-term solutions was always less than 0.01% at all values of $E/N < 2$ Td. This is a reflection of the isotropic nature of the velocity distribution function at these reduced electric fields. This is a consequence of the dominance of elastic scattering which is essentially isotropic nature, and as such collisions act to randomize the velocities with minimal changes in the speeds. This level of precision justifies the use of the two-term approximation in this reduced electric field regime, and all transport parameters quoted in this paper, unless stated otherwise, were computed with the two-term approximation.

B. Numerical representation of the cross section

As the present work is focussed on the comparisons with swarm parameters at a level of accuracy approaching 1% it is desirable to test the accuracy of the numerical representation of the cross sections. The cross sections used in the solution of the Boltzmann equation are typically given as a set of discrete points tabulated on a numerical grid [15, 17]. The density of grid points, and the approach used to interpolate between those points will have an impact upon the calculated transport parameters. This is evidenced by the fact that the improved numerical representations of vibrational cross sections did go some way towards reducing the discrepancies between vibrational cross sections derived from swarm and beam experiments [54].

The importance of the numerical representation of the cross section was tested by solving the Boltzmann equation with different tabulations of the same SDpT cross section. The SDpT cross sections use a high density tabulation with velocity increments of 0.001 a_0^{-1} near the $\epsilon = 0$ threshold. The SIGLO cross section has no cross section values below 0.030 eV. Removing all points below 0.03 eV from the SDpT tabulated cross section results in the 77 K $v_{\rm dr}$ at $E/N = 0.001594$ Td decreasing by 0.2% and the 77 K D_T/μ characteristic energy increasing by 8%. The characteristic energy is potentially much more sensitive to the numerical representation of the cross section than the drift velocity.

C. Comparison with drift velocities

Drift velocities at $T = 77$ K computed with the SDpT, SDpTv2, BSR and Buckman cross sections are compared with the measured ANU drift velocities in Table I. The SDpT v_{dr} utilized a multi-term solution of the Boltzmann equation and natural cubic spline interpolation was used to convert the tabulated values into a continuous function. All other calculations were done using the two-term approximation and linear interpolation. Table II compares the ANU $T = 293$ K $v_{\rm dr}$ [15] with those computed with the SDpT, SDpTv2, BSR and Buckman cross sections. The mean energy of the swarm at 77 K and 293 K is depicted in Figure 1 for applied reduced electric fields ranging from approximately 0.001 Td to 2.0 Td. The

TABLE I: Drift velocities, in units of 10^3 ms^{-1}, as a function of the reduced electric field, for electrons in neon at $T = 77$ K. The stated uncertainty for the ANU experimental drift velocities citerobertson72a is 1%.

E/N (Td)	SDpT [11]	SDpTv2	BSR [3, 7, 8]	Buckman [37]	ANU [15]
0.001594	0.4177	0.4258	0.3998	0.4245	0.424
0.002390	0.4994	0.5070	0.4884	0.5055	0.508
0.003187	0.5639	0.5700	0.5563	0.5693	0.572
0.003984	0.6180	0.6245	0.6117	0.6227	0.625
0.004781	0.6651	0.6711	0.6590	0.6691	0.671
0.005578	0.7072	0.7127	0.7007	0.7106	0.712
0.006374	0.7454	0.7504	0.7381	0.7481	0.751
0.007171	0.7805	0.7851	0.7724	0.7827	0.785
0.007968	0.8131	0.8173	0.8041	0.8148	0.817
0.01195	0.9499	0.9525	0.9354	0.9497	0.953
0.01594	1.060	1.061	1.040	1.058	1.062
0.01992	1.153	1.154	1.129	1.150	1.154
0.02390	1.235	1.236	1.208	1.232	1.235
0.03187	1.378	1.378	1.347	1.374	1.378
0.03984	1.501	1.501	1.468	1.496	1.500
0.04781	1.611	1.611	1.576	1.605	1.609
0.05578	1.711	1.711	1.674	1.704	1.707
0.06374	1.803	1.803	1.765	1.795	1.800
0.07171	1.889	1.889	1.850	1.881	1.885
0.07968	1.970	1.970	1.931	1.962	1.965
0.1195	2.325	2.324	2.281	2.315	2.320
0.1594	2.624	2.624	2.577	2.616	2.618
0.1992	2.888	2.888	2.839	2.883	2.883
0.2104	2.957	2.957	2.907	2.953	2.953
0.2390	3.126	3.126	3.075	3.125	3.125
0.3187	3.550	3.550	3.492	3.555	3.55
0.3984	3.921	3.921	3.856	3.932	3.92
0.4781	4.250	4.250	4.182	4.269	4.25
0.5259	4.432	4.432	4.362	4.455	4.44
0.5578	4.548	4.548	4.477	4.574	4.55
0.6374	4.819	4.819	4.746	4.853	4.82

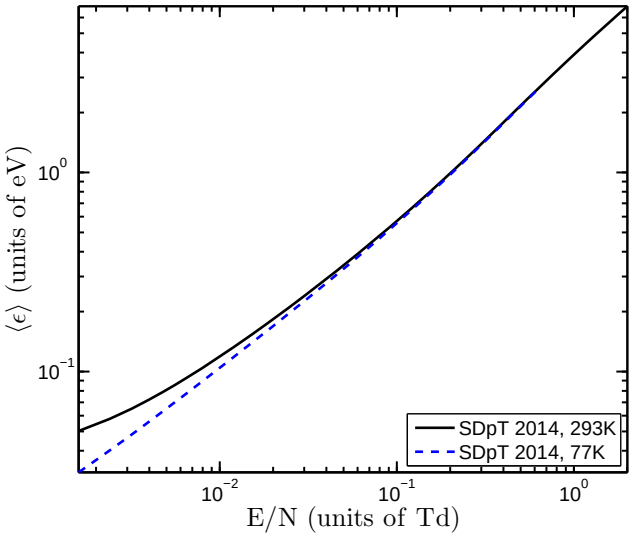

FIG. 1: (color online) The mean energy (in eV) as a function of E/N (in Td) for electron swarms in neon. The mean energy was computed using the SDpT cross section.

mean energies and swarm parameters for the two different temperatures are almost the same for $E/N > 0.03$ Td. The lowest mean energy for the 77 K data set occurs at 0.001594 Td and was 0.031 eV.

The SDpT $v_{\rm dr}$ tend to be slightly smaller (about 0.5-2%) than the 77 K ANU drift velocities for $E/N < 0.010$ Td. For larger values of E/N there are no instances of differences exceeding 1%. The SDpTv2 cross section, which has a smaller cross section below $\epsilon < 0.15$ eV, gives drift velocities that reproduce the ANU data with higher accuracy. Table III reports the root mean square (rms) of the relative difference between calculated and experimental transport parameters for a number of momentum transfer cross sections. The rms relative difference of the SDpTv2 cross section is four times smaller than the rms relative difference for the SDpT cross section. Another useful estimate of the accuracy is the largest relative difference between the calculated and measured transport parameters. These are listed in Table IV. This is 1.70% for the SDpT cross section, and 0.42% for the SDpTv2 cross section. The SDpTv2 cross section is in perfect agreement with the 77 K ANU transport data given that the stated experimental uncertainty is 1% [15].

Both the SDpT and SDpTv2 cross sections give almost the same drift velocities for the 293 K data set. The lowest value of E/N for the 293 K data set was 0.01518 Td. The lowest mean energy for this data set is about 0.05 eV, and at this energy the differences between the SDpT and SDpTv2 $\sigma_{\rm MT}$ are insignificant. The transport coefficients computed with these cross sections agree with the ANU $v_{\rm dr}$ to better than 0.5% for all $E/N < 1.5$ Td.

The SDpT and SDpTv2 transport parameters show substantial differences with the ANU data at $E/N = 1.821$ and 2.003 Td. The mean energy exceeds 5 eV when $E/N > 1.6$ Td and it is likely that excitations to the lowest energy excited states near 16.6 eV are starting to influence $v_{\rm dr}$ at the two largest values of E/N.

The discrepancies between the BSR $v_{\rm dr}$ and experiment are much larger, with a 5.7% discrepancy with the 77 K ANU drift velocity at $E/N = 0.001594$ Td and an rms difference of 2.2%. The BSR drift velocity is smaller than the ANU (and SDpT) drift velocities at all values of E/N which is indicative of a cross section which is too large. The BSR momentum transfer cross section is larger than the SDpT cross section for all energies below the first excitation threshold. The difference is especially significant at $\epsilon = 0$ eV where the BSR cross section is set to 0.500×10^{-20} m^2 (equivalent to a scattering length of 0.377 a_0) about 3 times larger than the SDpT cross

section. The BSR $\sigma_{\rm MT}$ is roughly constant for $\epsilon < 0.01$ eV, a functional dependence that is not compatible with MERT. The very large differences in the zero energy cross section do not lead to a commensurate change in the drift velocity because the cross section is so small at $\epsilon = 0$. The tendency for the BSR drift velocities to be smaller than experiment is also apparent in the 293 K data set.

TABLE II: Drift velocity, in units of 10^3 ms^{-1}, as a function of the reduced electric field, for electrons in neon at $T = 293$ K. The stated uncertainty for the ANU drift velocities is 1%.

E/N (Td)	SDpT [11]	SDpTv2	BSR [3, 7, 8]	Buckman [37]	ANU [15]
0.01518	0.9738	0.9756	0.9530	0.9721	0.976
0.01821	1.052	1.053	1.028	1.050	1.052
0.02125	1.122	1.123	1.096	1.119	1.122
0.02428	1.186	1.187	1.158	1.183	1.185
0.02732	1.246	1.246	1.216	1.242	1.243
0.03035	1.301	1.301	1.270	1.296	1.300
0.04553	1.536	1.536	1.501	1.530	1.532
0.06071	1.729	1.729	1.691	1.722	1.723
0.09106	2.046	2.046	2.005	2.038	2.040
0.1214	2.311	2.311	2.267	2.302	2.300
0.1518	2.544	2.544	2.498	2.536	2.532
0.1821	2.754	2.754	2.706	2.748	2.741
0.2125	2.948	2.948	2.897	2.944	2.935
0.2428	3.127	3.127	3.075	3.126	3.115
0.2732	3.297	3.297	3.241	3.298	3.284
0.3036	3.456	3.456	3.398	3.460	3.445
0.3643	3.750	3.750	3.688	3.759	3.738
0.4250	4.018	4.018	3.952	4.033	4.004
0.4553	4.144	4.144	4.076	4.161	4.130
0.4857	4.264	4.264	4.195	4.284	4.255
0.5464	4.492	4.492	4.421	4.518	4.478
0.6071	4.704	4.704	4.632	4.736	4.699
0.7589	5.178	5.178	5.105	5.226	5.170
0.9106	5.589	5.589	5.517	5.654	5.576
1.062	5.954	5.594	5.883	6.033	5.945
1.214	6.284	6.284	6.216	6.377	6.280
1.336	6.529	6.529	6.462	6.631	6.542
1.821	7.377	7.377	7.317	7.509	7.813
2.003	7.659	7.659	7.601	7.799	8.491

The Buckman cross section is based on the original momentum transfer cross section of Robertson [15]. As expected, this cross section does a uniformly good job of reproducing the measured drift velocities at almost all values of E/N. The rms difference of this momentum transfer cross section with the 77 K and 293 K drift velocity data is less than 1%. The Buckman cross section does tend to be about 1% larger than the ANU drift velocity for $E/N > 0.6$ Td.

The *ab-initio* MCHF $\sigma_{\rm MT}$ gives larger rms differences with the ANU drift velocities than the SDpT or SDpTv2 cross sections. The larger rms difference is partly due to incomplete information about its behaviour at higher energies.

TABLE III: The rms relative difference between experimental and calculated transport parameters. The $E/N = 1.821$ and 2.003 Td $v_{\rm dr}$ are not part of the error calculation for the 293 K data set.

Set	$v_{\rm dr}$ 77 K [15]	$v_{\rm dr}$ 293 K [15]	D_T/μ [17]
SDpT [11]	0.00618	0.00295	0.0253
BSR [3, 7, 8]	0.0221	0.0163	0.0132
MCHF [35]	0.00542	0.00819	0.0239
SDpTv2	0.00146	0.00296	0.0333
SIGLO [3, 43]	0.00143	0.00209	0.0318
Buckman [37]	0.00324	0.00718	0.0278
Morgan [3, 42]	0.00369	0.00154	0.0366
Biagi v8.9 [3, 47, 48]	0.00299	0.00285	0.0303
Puech [3, 49, 50]	0.0143	0.0104	0.0157

The SIGLO, Morgan and Biagi cross sections accurately reproduce the ANU drift velocity to a high degree of accuracy, and the largest rms difference resulting from any of these cross sections is less than 0.4%. This is not surprising since all three cross section sets are based on the Robertson [15] or O'Malley [21] cross sections at low energies with some fine tuning occurring at energies greater than 4 eV.

D. Comparison with the characteristic energy, D_T/μ

Table V gives the characteristic energy, D_T/μ, for a swarm travelling through neon gas at $T = 293$ K. Experimental data comes from the Rikkyo group [17]. The key conclusion to be drawn from the Table V is that there is a 3% discrepancy at the level of the transport coefficients between cross sections that reproduce drift velocity measurements and cross sections that reproduce the Rikkyo data for the transverse diffusion coefficients.

The SDpT D_T/μ tend to be larger than the Rikkyo data. The rms difference is 2.5% with the largest difference being 3.5%. The largest differences tend to occur at the smallest values of E/N. This is clearly visible in Figure 2 where the relative difference is given. The SDpT cross section would need to be increased in order to be compatible with the Rikkyo experiment. However, the SDpTv2 $\sigma_{\rm MT}$ is actually smaller than the SDpT $\sigma_{\rm MT}$. Hence the rms difference of the SDpTv2 transport parameters with the Rikkyo data has increased to 3.3%. Figure 2 shows that the increase in the difference with the Rikkyo data is most prominent at the lowest E/N.

Four of the empirical cross sections, the Buckman, SIGLO, Morgan and Biagi cross sections have rms differences that range from 2.8% to 3.7%. These cross sections

TABLE IV: The maximum relative difference between experimental and calculated transport parameters. The relative difference is given above the value of E/N at which it occurs. The E/N at 1.821 and 2.003 Td at 293 K were excluded from consideration.

Set	$v_{\rm dr}$ 77 K [15]	$v_{\rm dr}$ 293 K [15]	D_T/μ [17]
SDpT	0.0170	0.00477	0.0346
	0.002390	0.1214	0.014
BSR [3, 7, 8]	0.0571	0.0236	0.0237
	0.001594	0.01518	0.35
MCHF [35]	0.0101	0.0180	0.0391
	0.002390	1.214	0.014
SDpTv2	0.00417	0.00475	0.0553
	0.001594	0.1214	0.014
SIGLO [3, 43, 44]	0.00301	0.00380	0.0530
	0.5259	0.2732	0.014
Buckman [37]	0.00694	0.0154	0.0507
	0.6374	1.214	0.014
Morgan [3, 42]	0.00817	0.00310	0.0639
	0.007968	0.01518	0.014
Biagi v8.9 [3, 47, 48]	0.00502	0.00523	0.0591
	0.003187	1.336	0.014
Puech [3, 49, 50]	0.0380	0.0171	0.0267
	0.001594	0.2732	0.30

give a D_T/μ that exceeds experiment in all cases. The inherent discrepancy between the drift velocity and diffusion data are clearly seen in Table III. The cross section sets that have less than 0.5% rms discrepancy with the drift velocity data all have greater than 3% rms relative differences with the diffusion data.

The BSR cross section gives a smaller rms difference with the Rikkyo data than the other two *ab-initio* cross sections. The BSR cross section is larger than these other cross sections and this results in smaller values of D_T/μ. The BSR D_T/μ are mostly 1-2% too small over the entire range of E/N. However, the relative difference of all values of BSR D_T/μ lie within the stated uncertainty of 3%. One feature of the graph is the 1.6% jump that occurs between 0.30 and 0.35 Td.

The Puech cross section has rms differences with the $v_{\rm dr}$ and D_T/μ data of 1.0 to 1.5%. This suggests that this cross section has been constructed to give equally good fits to both the $v_{\rm dr}$ and D_T/μ transport data.

The cross sections that give the better than 0.5% accuracy fits to the ANU drift velocities give rms differences of 3% with the D_T/μ data. This does not constitute an irreconcilable conflict since the stated uncertainty in the Rikkyo measurements was 3%. However, one aim of the present paper is to test the quality of various momentum transfer cross sections at a 1% level of precision. Consequently, precedence should be given to fitting ANU $v_{\rm dr}$ data ahead of Rikkyo D_T/μ data.

TABLE V: The characteristic energy D_T/μ, (in eV) with electric field (in Td), for electrons in neon at $T = 293$ K. The stated uncertainty of the Rikkyo data is 3%.

E/N (Td)	SDpT [11]	SDpTv2	BSR [3, 7, 8]	Buckman [37]	Rikkyo [17]
0.014	0.1314	0.1340	0.1268	0.1334	0.127
0.017	0.1491	0.1518	0.1442	0.1511	0.146
0.020	0.1660	0.1687	0.1606	0.1679	0.162
0.025	0.1926	0.1953	0.1864	0.1943	0.187
0.030	0.2177	0.2204	0.2105	0.2193	0.213
0.035	0.2418	0.2444	0.2336	0.2431	0.236
0.040	0.2649	0.2674	0.2557	0.2660	0.260
0.050	0.3091	0.3115	0.2978	0.3098	0.300
0.060	0.3511	0.3533	0.3379	0.3513	0.341
0.070	0.3914	0.3935	0.3764	0.3911	0.382
0.080	0.4304	0.4324	0.4137	0.4297	0.420
0.10	0.5054	0.5072	0.4856	0.5038	0.491
0.12	0.5774	0.5791	0.5549	0.5750	0.562
0.14	0.6473	0.6488	0.6221	0.6440	0.630
0.17	0.7492	0.7506	0.7204	0.7449	0.730
0.20	0.8486	0.8499	0.8165	0.8435	0.828
0.25	1.011	1.012	0.9733	1.005	0.987
0.30	1.169	1.170	1.127	1.163	1.14
0.35	1.326	1.327	1.279	1.320	1.31
0.40	1.480	1.481	1.429	1.476	1.46

E. Comparison with the thermal diffusion coefficient

The thermal diffusion coefficient for electrons diffusing in neon has been measured on a number of occasions [23–26]. Discounting some earlier measurements, estimates have been made at Oak Ridge National Laboratory (ORNL) [24], the Laboratori C. I. S. E [22, 23] and the ANU [25, 26]. The C.I.S.E. value of ND is converted from the stated diffusion constant of $D_0 = (2860 \pm 100)$ cm^2 s^{-1} [23] by assuming that measurements were taken at a gas temperature of 273 K.

The three experimental diffusion constants are not compatible within their mutual experimental uncertainties when temperature dependent effects are taken into consideration. Preference is given to the ANU value of ND.

Comparisons of experimental diffusion coefficients, ND with calculations using the SDpT and BSR cross section sets can be found in Table VI. The mean energy of a thermal electron cloud at 295 K is 0.0381 eV. The ND diffusion coefficient varies slowly with temperature. For example, using the SDpTv2 cross section and decreasing the temperature results in ND decreasing from 75.04×10^{20} mm^{-1} s^{-1} to 74.14×10^{20} mm^{-1} s^{-1}, a change of only 1.2%.

The good agreement between the MCHF and ANU

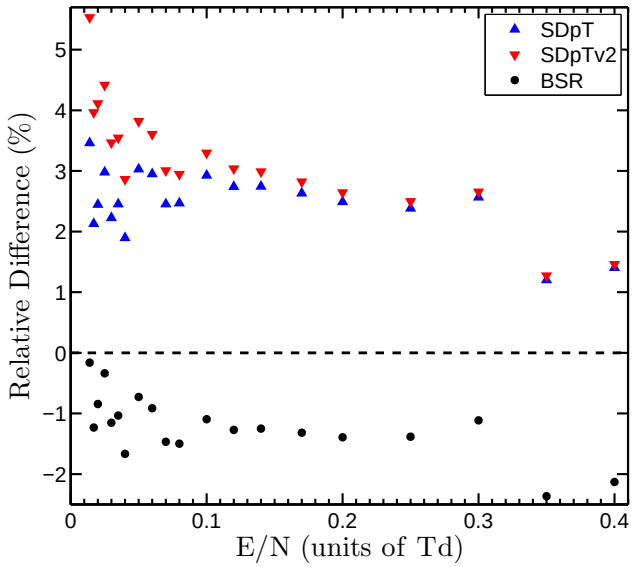

FIG. 2: (color online) The relative difference, between calculated characteristic energies and the experimental data of the University of Rikkyo [17] group.

TABLE VI: The thermal diffusion coefficient, ND, in units of 10^{20} mm^{-1} s^{-1}, for thermal electrons in neon gas.

Source	ND	
	$T = 295$ K	$T = 273$ K
ORNL [24] ($T = 300$ K)	64.7	
Laboratori C.I.S.E [23, 25, 26]		76.9 ± 2.4
ANU [25]	$72.7^{+2.0}_{-0.9}$	
SDpT [11]	71.28	70.36
BSR [3, 7, 8]	59.51	58.05
MCHF [35]	72.73	71.81
SDpTv2	75.04	74.14
SIGLO [3, 43, 44]	77.61	77.01
Buckman [37]	74.68	73.81
Morgan [3, 42]	75.93	75.13
Biagi v8.9 [3, 47, 48]	79.97	79.48
Puech [3, 49, 50]	66.47	65.41

ND coefficients suggests that the ANU diffusion experiment would be consistent with a scattering length that is close to the MCHF calculation, namely 0.2218 a_0 [35]. The SDpTv2 value of ND of 75.04×10^{20} mm^{-1} s^{-1} lies just outside the error bounds for the ANU measurement.

One of the issues affecting comparisons with the empirically derived cross sections such as the SIGLO, Morgan and Biagi is their numerical representation. These cross sections all have relatively few tabulated points below 0.1 eV where the cross section changes by a factor of 4. This had an impact of 1-4% on the calculated diffusion constant. A significant part of the differences between the ND values of the Buckman, SIGLO, Morgan and Biagi values of ND arises from the energies at which the cross sections are tabulated.

The BSR cross section gives a diffusion coefficient of 59.5×10^{20} mm^{-1} s^{-1}, about 20% lower than the ANU value. This underestimate further illustrates the problems with the BSR cross section at energies below 0.15 eV.

One of the salient conclusions drawn from Table VI is the overall degree of consistency between the Buckman, SDpTv2, MCHF and ANU values of ND. The Buckman and SDpTv2 cross section give very similar drift velocities that are close to ANU values [15]. These are effectively compatible with the ANU ND within the experimental uncertainty.

There is one other electron transport parameter that has been measured for neon, the longitudinal diffusion coefficient on mobility, D_L/μ [16]. However, the lowest value of E/N for which measurements have been made is 1.4 Td and the effects of inelastic collisions could make a contribution here. Consequently, no calculations of the longitudinal diffusion parameter were made.

F. Recommended low energy momentum transfer cross section

Two measures have been given as metrics to test the performance of the different cross sections against the drift velocity and transverse diffusion data. These are the root mean square of the relative difference between the calculated and measured transport parameters and secondly the largest relative difference between the calculated and measured transport parameters.

The SIGLO momentum transfer cross section gives drift velocities with very small rms difference from the ANU experiment of 0.14% at 77 K and 0.21% at 293 K, which are slightly smaller than those using the SDpTv2 cross section. Despite these very low differences from ANU drift velocity data, in many aspects the SDpTv2 cross section has one significant advantage over the SIGLO cross section. For example, the SDpTv2 diffusion constant, ND, is closer to the ANU experimental value than the SIGLO value of ND. The smaller rms difference of the SIGLO values of $v_{\rm dr}$ is of minor importance since all of the SIGLO and SDpTv2 values of the drift velocity lie within the stated 1% uncertainty. However, the SDpTv2 cross section, being derived from a large *ab-initio* calculation, has a functional dependence based on a properly founded dynamical description of the electron-neon interaction as opposed to the SIGLO cross section which like other purely empirical cross sections is a table of numerical values constructed to fit experimental values of the drift velocity. In effect, the SDpTv2 $\sigma_{\rm MT}$ varies smoothly as a function of energy in a manner that can be expected to be consistent with the actual momentum transfer cross section.

V. CONCLUSION

A high precision comparison of transport parameters computed with various low energy electron-neon cross sections is presented. The use of the two-term approximation is justified and the error associated with its usage is determined to be less than 0.01%. One novel feature is the comparison with the thermal energy diffusion coefficient from the ANU group [25, 26]. Direct comparisons of theoretical cross sections with measured transport parameters (as opposed to the momentum transfer cross section) is still relatively rare.

One major conclusion pertains to the relatively high degree of precision achieved by the three *ab-initio* momentum transfer cross sections. The SDpT $\sigma_{\rm MT}$ gives drift velocities that have an rms difference with the ANU drift velocity data of only 0.62% and 0.30% for the 77 K and 293 K $v_{\rm dr}$ data respectively. The only significant differences for the SDpT cross section occur for very low E/N and even here the largest difference is only 1.7%.

The BSR cross section gave a poorer fit to the drift velocity data, but even here the rms discrepancies are only about 2%.

The low energy imperfections in the SDpT $\sigma_{\rm MT}$ were removed by performing an energy dependent scaling of the SDpT $\sigma_{\rm MT}$. This reduced the rms differences with the ANU $v_{\rm dr}$ data to 0.15% and 0.30% at 77 K and 293 K respectively. There was no instance of a discrepancy greater than 0.5% for drift velocity data below 1.4 Td. This cross section, being derived from a high quality treatment of e^--neon scattering has the advantage of a smooth energy dependence that can be expected to closely conform to that of the actual momentum transfer cross section.

In some respects the present investigation complements the previous cross section assessment of Alves *et al.* [3]. The Alves *et al.* investigation was aimed at assessing e^--neon cross section compilations for modelling low temperature plasmas. An acceptable level of accuracy would be better than 10% in the most common transport parameters. The present assessment is best summarized as a test of low energy momentum transfer cross sections with the expected level of accuracy in the computed transport parameters being less that 1%. Critical comparisons of the fine details of different *ab-initio* cross sections require this high degree of accuracy.

Acknowledgments

This work was supported under the Australian Research Council's (ARC) Centre of Excellence program.

[1] K. Bartschat, E. T. Hudson, M. P. Scott, P. G. Burke, and V. M. Burke, J. Phys. B **29**, 2875 (1996).
[2] D. V. Fursa and I. Bray, J. Phys. B **30**, 757 (1997).
[3] L. L. Alves, K. Bartschat, S. F. Biagi, M. C. Bordage, L. C. Pitchford, C. M. Ferreira, G. J. M. Hagelaar, W. L. Morgan, S. Pancheshnyi, A. V. Phelps, et al., J. Phys. D **46**, 334002 (2013).
[4] O. Zatsarinny and K. Bartschat, J. Phys. B **47**, 061001 (2014).
[5] R. K. Nesbet, Phys. Rev. A **20**, 58 (1979).
[6] S. J. Buckman and M. J. Brunger, Aust. J. Phys. **50**, 483 (1997).
[7] O. Zatsarinny and K. Bartschat, Phys. Rev. A **85**, 062710 (2012).
[8] O. Zatsarinny and K. Bartschat, *BSR database* (2014), URL `http://www.lxcat.net/`.
[9] M. S. Safronova, W. R. Johnson, and A. Derevianko, Phys. Rev. A **60**, 4476 (1999).
[10] M. S. Safronova and W. R. Johnson, Adv. At. Mol. Opt. Phys. **55**, 191 (2008).
[11] Y. Cheng, L. Y. Tang, J. Mitroy, and M. S. Safronova, Phys. Rev. A **89**, 012701 (2014), URL `http://link.aps.org/doi/10.1103/PhysRevA.89.012701`.
[12] R. A. Nielsen, Phys. Rev. **50**, 950 (1936).
[13] J. C. Bowe, Phys. Rev. **117**, 1411 (1960).
[14] J. L. Pack and A. V. Phelps, Phys. Rev. **121**, 798 (1961).
[15] A. G. Robertson, J. Phys. B **5**, 648 (1972).
[16] H. N. Kucukarpaci, H. T. Saelee, and J. Lucas, J. Phys. D **14**, 9 (1981).
[17] T. Koizumi, H. Murakoshi, S. Yamamoto, and I. Ogawa, J. Phys. B **17**, 4387 (1984).
[18] L. S. Frost and A. V. Phelps, Phys. Rev. **136**, 1538 (1964).
[19] R. O. Berger, T. F. O'Malley, and L. Spruch, Phys. Rev. **137**, 1068 (1965).
[20] P. S. Hoeper, W. Franzen, and R. Gupta, Phys. Rev. **168**, 50 (1968).
[21] T. F. O'Malley and R. W. Crompton, J. Phys. B **13**, 3451 (1980).
[22] G. Cavalleri, E. Gatti, and P. Principi, Nuovo Cimento **31**, 318 (1964).
[23] G. Cavalleri, E. Gatti, and A. M. Interlenghi, Nuovo Cimento B Serie **40**, 450 (1965).
[24] D. R. Nelson and F. J. Davis, J. Chem. Phys. **51**, 2322 (1969).
[25] T. Rhymes, R. W. Crompton, and G. Cavalleri, Phys. Rev. A **12**, 776 (1975).
[26] T. Rhymes, R. W. Crompton, and G. Cavalleri, Phys. Rev. A **14**, 898 (1976).
[27] J. L. Pack, R. E. Voshall, A. V. Phelps, and L. E. Kline, J. Applied Physics **71**, 5363 (1992).
[28] L. G. H. Huxley and R. W. Crompton, *Diffusion and drift of electrons in gases* (Wiley, New York, 1974).
[29] R. D. White, R. E. Robson, B. Schmidt, and M. A. Morrison, J. Phys. D **36**, 3125 (2003).
[30] R. P. McEachran and A. D. Stauffer, Aust. J. Phys. **50**, 511 (1997).
[31] T. F. O'Malley, Phys. Rev. **125**, 1300 (1962).
[32] T. F. O'Malley, Phys. Rev. **130**, 1020 (1963).
[33] S. J. Buckman and J. Mitroy, J. Phys. B **22**, 1365 (1989).
[34] Supplementary material giving tables of SDpT and SDpTv2 cross sections on a fine energy grid.

[35] H. P. Saha, Phys. Rev. Lett. **65**, 2003 (1990).
[36] S. Pancheshnyi, S. Biagi, M. C. Bordage, G. J. M. Hagelaar, W. L. Morgan, A. V. Phelps, and L. C. Pitchford, Chem. Phys. **398**, 148 (2012).
[37] S. J. Buckman and M. T. Elford, *Momentum transfer cross sections*, pp. 2–35, in [38] (2000).
[38] Y. K. Itikawa, ed., *Photon and Electron Interactions with Atoms, Molecules and Ions* (Springer, Berlin, 2000).
[39] D. F. Register and S. Trajmar, Phys. Rev. A **29**, 1785 (1984).
[40] R. J. Gulley, D. T. Alle, M. J. Brennan, M. J. Brunger, and S. J. Buckman, J. Phys. B **27**, 2593 (1994).
[41] H. P. Saha, Phys. Rev. A **39**, 5048 (1989).
[42] W. L. Morgan, *Morgan (Kinema Research and Software) database,* (2014), URL `http://www.lxcat.net/`.
[43] J. Meunier, P. Belenguer, and J. P. Boeuf, J. Applied Physics **78**, 731 (1995).
[44] L. C. Pitchford and J. P. Bouef, *The SIGLO database* (2014), URL `http://www.lxcat.net/`.
[45] I. Shimamura, Sci. Papers Inst. Phys. Chem. Res. **82**, 1 (1989).
[46] S. F. Biagi, Nucl. Instr. and Meth. A **283**, 716 (1989).
[47] S. F. Biagi, *Magboltz - transport of electrons in gas mixtures* (2012), URL `http://consult.cern.ch/writeup/magboltz/`.
[48] S. F. Biagi, *Biagi database* (2014), URL `http://www.lxcat.net/`.
[49] V. Puech and S. Mizzi, J. Phys. D **24**, 1974 (1991).
[50] V. Puech, *Puech database* (2014), URL `http://www.lxcat.net/`.
[51] L. Boltzmann, Weiner Berichte **66**, 275 (1872), [(1909) Wissenschaftliche Abhandlungen **1** 316].
[52] R. D. White, R. E. Robson, S. Dujko, P. Nicoletopoulos, and B. Li, J. Phys. D **42**, 194001 (2009).
[53] D. R. Lide, ed., *CRC Handbook of Chemistry and Physics*, vol. 88 (CRC Press, Boca Raton, Florida, 2008).
[54] B. Schmidt, K. Berkhan, B. Gotz, and M. Muller, Phys. Scr. **T53**, 30 (1994).